Two-wavelength whole-field interferometry setup for thermal lens study

Danilo M. Silva*[a], Eduardo A. Barbosa[b], Niklaus U. Wetter[a]
[a] Instituto de Pesquisas Energéticas e Nucleares (CNEN-IPEN/SP), CEP 005508-000 São Paulo, Brazil;
[b] Laboratório de Óptica Aplicada, Faculdade de Tecnologia de São Paulo, CEETEPS-UNESP, Pça Cel Fernando Prestes, 30, CEP 01124 060, São Paulo, Brazil

ABSTRACT

In this paper we present a new approach for thermal lens analysis using a two-wavelength DSPI (Digital Speckle Pattern Interferometry) setup for wavefront sensing. The employed geometry enables the sensor to detect wavefronts with small phase differences and inherent aberrations found in induced lenses. The wavefronts was reconstructed by four-stepping fringe evaluation and branch-cut unwrapping from fringes formed onto a diffusive glass. Real-time single-exposure contour interferograms could be obtained in order to get discernible and low-spacial frequency contour fringes and obtain low-noise measurements. In our experiments we studied the thermal lens effect in a 4% Er-doped $CaO\text{-}Al_2O_3$ glass sample. The diode lasers were tuned to have a contour interval of around 120 μm. The incident pump power was longitudinally and collinearly oriented with the probe beams. Each interferogram described a spherical-like wavefront. Using the ABCD matrix formalism we obtained the induced lens dioptric power from the thermal effect for different values of absorbed pump power.
Keywords: Speckle, thermal lens, multi-wavelength, wavefront sensing, laser

1. INTRODUCTION

Thermal effects are often a limiting factor in solid-state lasers research when designing optical resonators and systems, affecting the stability, efficiency, oscillating mode sizes, optical beam quality and output power of lasers or power throughput of optical systems[1]. Especially when the thermal lens assumes a non-symmetrical form such as common spherical or aspherical lens shape, more sophisticated techniques are necessary to determine the thermal lens. Only after knowing the exact shape, effective countermeasures can be taken in order to minimize or even eliminate the detrimental effects caused by the thermal distortion and index change of the optical components[2,3].
Several techniques have been used to describe and quantify optical damage and distortions in photonic materials. Among the most employed we can mention the Shack-Hartmann aberrometer (SH), which evaluates the incident wave phase through a microlens array placed in front of a CCD target. The phase is determined by measuring the displacements undergone by each spot focused onto the CCD. The SH has been applied in many fields like ophthalmology, quality control in lens fabrication and astronomy[4]. This vibration-imune wavelength-independent device presents other important characteristics like simplicity, robustness, and compactness.

The purpose of this work is to introduce speckle pattern interferometry with two wavelengths as an alternative method to study thermal lensing in optical resonators. In our setup the probe beam illuminates a diffusive glass plate (DGP) after passing through the thermally stressed photonic sample. Due to the two-wavelength DSPI process the speckled DGP image appears modulated by interference contour fringes describing the incident wavefront geometry, as reported elsewhere[5]. By properly changing the optical path of this wave, we can use phase retrieval algorithms to reconstruct the wavefront. The introduction of DSPI made wavefront reconstruction processes more sophisticated, accurate and versatile[6,7] and provides high spatial resolution. Digital speckle pattern interferometry (DPSI) has demonstrated to be a suitable technique for non-destrutive testing and whole-field analysis from light transmitted through the sample, thus providing information from each part of studied medium. Typically the spatial resolution of speckle methods depends on the pixel size of the camera of the order of 5 μm, which is significantly higher than the SH resolution, limited by the

Speckle 2012: V International Conference on Speckle Metrology, edited by
Ángel F. Doval, Cristina Trillo, J. Carlos López-Vázquez, Proc. of SPIE Vol. 8413, 841319

distance between the microlenses, usually around 100 μm. Further advantage remains on the possibility to adapt the interferometer configuration setup for specific conditions. Thereby, DPSI have been applied in many fields of knowledge like microscopy, profilometry, for mechanical properties investigation like material under strain, heat or harmonic vibration when different states taken from the object are compared[5].

This work describes the development of a dual-wavelength speckle interferometer to characterize the thermal lens effect in photonic samples by measuring the change in the wavefront geometry of a probe beam. Interferograms were obtained from the interference between reference wave and the object wave constituted by at a diffusively glass plate in order to get the speckle pattern. We used the four stepping technique and branch-cut method to reconstruct the wavefront at the sample. The studied sample was an Er-doped CaO-Al_2O_3 glass pumped by a 1.8 W diode laser emitting at 974 nm.

2. MULTIWAVELENGTH DSPI

Consider the interference between the object (S) and reference (R), both originating from two diode lasers emitting at the wavelengths λ_1 and λ_2 and having the same propagation direction. The object and reference beams at the CCD target are written as

$$R_N = R_0\left(e^{i(k_1\Gamma_R+\phi_1)} + e^{i(k_2\Gamma_R+\phi_2)}\right)$$
$$S_N = S_0\left(e^{i\left(k_1\Gamma_{S(x,y)}+\phi_1\right)} + e^{i\left(k_2\Gamma_{S(x,y)}+\phi_2\right)}\right) \quad (1)$$

where $k_{1,2} = 2\pi/\lambda_{1,2}$ are wave numbers, ϕ_1 and ϕ_2 are phases at the lasers output, $\Gamma_S(x,y)$ is the object wave path through a point(x,y)on the glass plate and Γ_R is the optical path of the reference wave. Interference occurs between the plane reference wave and the scattered light from the diffusive surface. The resulting signal formed at the detector is a fringe pattern with low-spatial frequency describing the object shape, and a high-spatial frequency speckle distribution due to scattering. In order to enhance the modulated contour fringes and eliminate the background due to the reference beam the subtractive method was employed[4], resulting in the interferogram shown in figure 1a .After applying a Fast Fourier Transform to retrieve low-frequency component shown in figure 1b, the interferogram signal V takes the form[7]

$$V(x,y) = V_0\cos^2\left[\frac{\pi}{\lambda_S}(\Gamma_S(x,y) - \Gamma_R)\right] \quad (2)$$

where $V_o \propto R_0S_0$ and $\lambda_S \equiv \lambda_1\lambda_2/|\lambda_1 - \lambda_2|$ is the synthetic wavelength. Equation (2) was obtained by taking into account that the phase difference $\phi_1 - \phi_2$ has a random behaviour[8]. This interferogram describes the surface shape moiré-like fringes acting as topographic contour lines. From equation 2 we can determine the spacing between two consecutive planes Δz, or contour interval as

$$\Delta z = \frac{\lambda_1\lambda_2}{|\lambda_1-\lambda_2|} \equiv \lambda_S \quad (3)$$

Once the separation of the wavelength $\lambda_1 - \lambda_2$ is known, a proper setting of the emitted wavelengths allows the contour interval to be adjusted. This does enable a change in the interferogram spatial frequency and consequently better fringe visibility and sensitivity enhancement.

The wavefront was 3D reconstructed by means of fringe evaluation through the four-stepping procedure. In this method four interferograms are sequentially phase-shifted and their intensities are combined in order to obtain the phase map, according to

$$\phi_{4-step} = \arctan\left(\frac{V_3 - V_1}{V_0 - V_2}\right) \quad (4)$$

The branch-cut method[9] was used as unwrapping technique to deconvolute the phase map and reconstruct the wavefront.

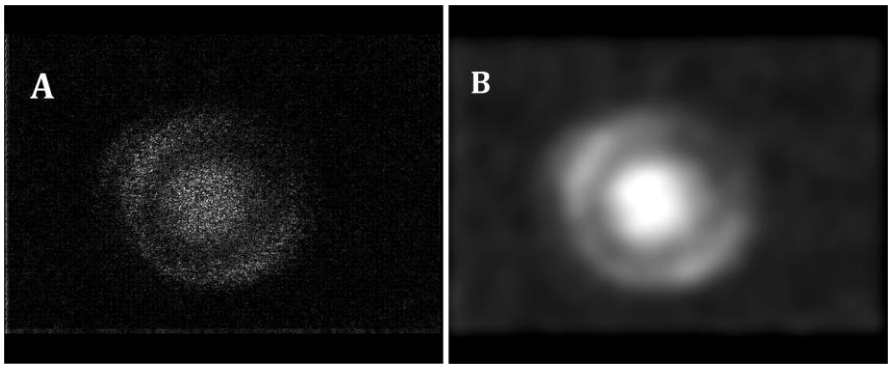

Figure 1: A- Speckle interferogram; B- Low-pass filtered interferogram

3. FOCAL LENGTH MEASUREMENT

The effect of induced thermal lens in photonic materials arises from heat due to non-radioactive relaxations after absorption of radiation. Some mechanisms are related to that effect, like a transverse gradient of refractive index dn/dT caused by temperature gradient throughout the sample, or mechanical stress bulges the end faces of the sample. The induced lens is more pronounced with higher incident power.

We opted for a configuration that overlaps of the idler imaging beam and the pump beam, by matching both beam waists and positioning them at the same plane where the sample was placed, as schematized in figure 1. The pump diode laser with emission centered near to the absorption peak of the sample (980 nm) focuses almost all its energy at the center of the material and generates sufficient heat to induce mechanical stresses. With the help of a dichroic mirror the idler beam originated from the red diode lasers was used as the object beam, as shown in figure 2.

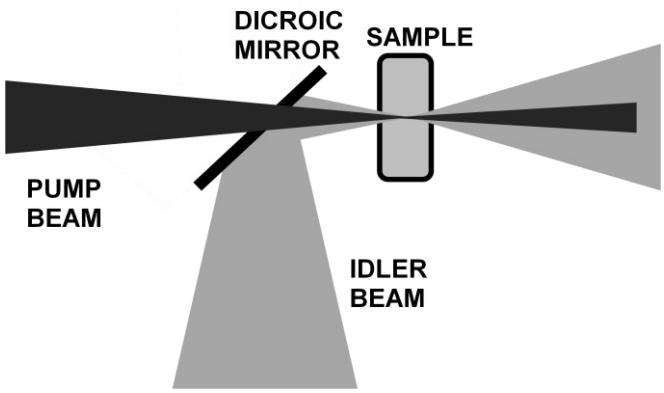

Figure 2: Induced thermal lens setup

The dicroic mirror is highly transmitting for the pump laser wavelength and highly reflective to the idler beam wavelength. Increasing incident pump power results in changes in the wavefront of the idler beam due to thermal lensing, which can be observed as the concentric contour fringes move. Figure 3 shows the whole setup.
We derived the focal length expression using the ABCD matrix formalism, considering a Gaussian beam described by $1/q_i = 1/R_i - i\lambda/\pi\omega_i^2$, where R_i is curvature radius of the wavefront and ω_i is the beam radius at plane i.
The beam parameters q_1 at the input of lens L1 and q_2 at the output of lens L2 shown in figure 3 are related according to[10].

$$\frac{1}{q_2} = \frac{C + D/q_1}{A + B/q_1} \tag{5}$$

The optical elements ensembles are described by the matrix elements *A, B, C* and *D*. We have a planar wave impinging lens L1, so that $1/R_1 = 0$. Thus, the curvature radius R_2 after passing through lens L2 is

$$\frac{1}{R_2} = \frac{ACb_1^2 + BD}{A^2 b_1^2 + B^2} \tag{6}$$

The focal length of the induced lens f_{TL} is thus given by

$$f_{TL} = \frac{\left(\frac{x}{f_1} - 1\right)\left[R_2\left(1 - \frac{L-x}{f_2}\right) - L + x\right]}{1 - \frac{L}{f_1} + \frac{R_2}{F}} \tag{7}$$

where $F^{-1} \equiv 1/f_1 + 1/f_2 - L/(f_1 f_2)$ is the optical power of the system without the thermal lens. By determining the curvature R_2 and distance x of sample from L1, one can easily obtain the induced focal length from equation 7.

4. EXPERIMENTS

The thermal lens measurement of a 4% Er-doped $CaO\text{-}Al_2O_3$ glass sample was undertaken by evaluating changes in wavefront curvature after scaling pump power at the sample. The images were obtained with the DPSI setup schematized in figure 3. The diode lasers emitting at 656,52 nm and 657,70 nm were aligned to have the same propagation direction. They were divided by beam splitter BS1 into two arms of the interferometer. The reference beam passed through spatial filter SF and was collimated by lens L3, impinging the CCD device through beam splitter BS2.

The study of thermal lensing was performed in the object arm of interferometer. Our pump system was composed by fiber-coupled diode laser with CW emission at 974 nm and a 2-cm focal length lens resulting in a beam waist of 230 μm. The idler beam was projected with a collimating system formed by lens L1 and L2 with focal lengths 2,5 cm and 26 cm, respectively. The sample was positioned near lens L1 focus in order to match the idler beam and the pump beam modes, thus providing a good measurement sensitivity. The diffusive glass plate DGP was positioned in front of L2 and a piezoeletric transducer PZT vibrating at 4 Hz was attached to the dichroic mirror DM in order to enable fringe visualization and interferogram processing[5]. The acquired images displayed the DGP covered by contour fringes. The four-stepping method was performed by applying displacements on mirror M3 with steps of 30 μm due to the 120-μm synthetic wavelength. The CCD camera was a Sony SSC-C104 and the objective lens L4 that formed the images onto the CCD device has a 5-cm focal length and a stop with an aperture of 9mm. An IR-filter was used in front of the camera to avoid CCD damage.

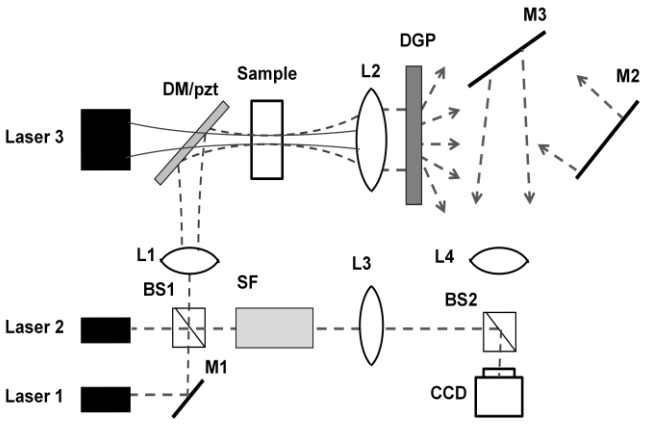

Figure 3: DPSI optical setup

5. RESULTS

Initially the absorbed pump power was measured as a function of the pump laser drive current, presenting a slope efficient of 40%. The wavefront was then reconstructed for each measured pump power. The measurements started after the stabilization of the fringes when thermal equilibrium was achieved. Figure 5a shows a result of a phase map retrieved through the four-step method and figure 5b shows the reconstructed wavefront after phase unwrapping.

The results presented a smooth profile what suggests that a parabolic fitting is a good choice to take the curvature radius in order to calculate the focal length. In figure 6a we have a parabolic profile extracted from figure 5b with the drawn solid line. The calculated curvature is shown in table 1.

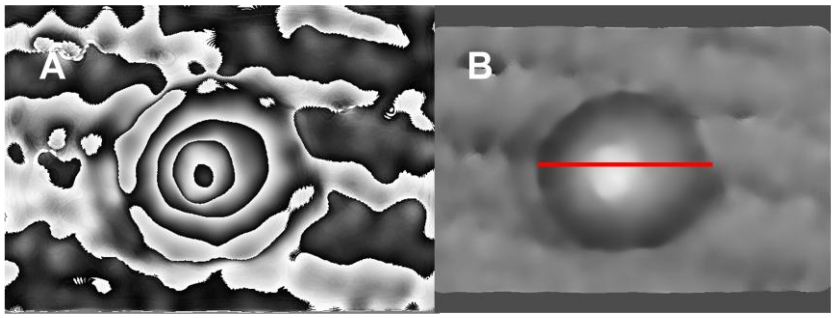

Figure 4: A- Phase-map interferogram, B- Unwrapped interferogram

In figure 6b the focal length is plotted for different values of pump power. We can observe a linear behavior and a decrease of focal length with increasing energy deposited in the sample, which is a very common behavior in materials with positive thermal conductivity[11]. The thermal conductivity for calcium aluminate glass is$\sim 1{,}55\ W/mK$.

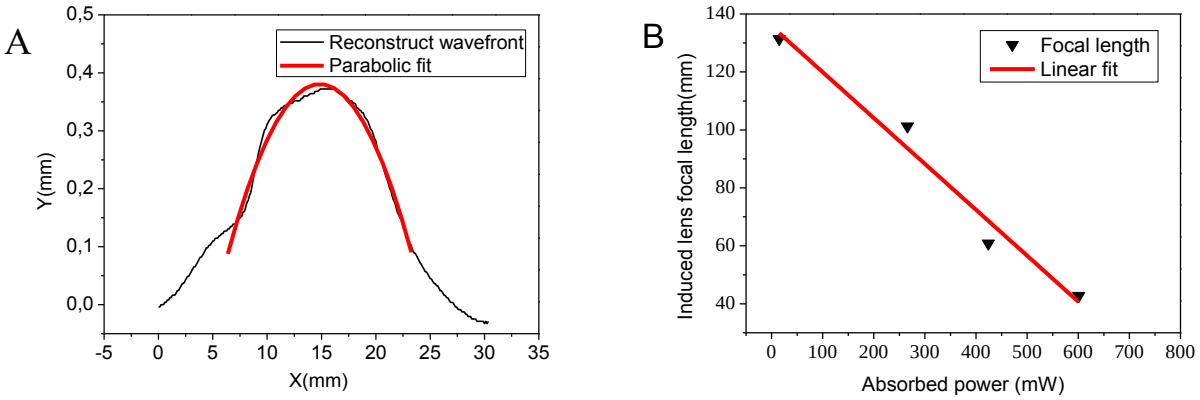

Figure 5: A-Wavefront profile with parabolic fitting, B- Quantitative thermal lens focal length

Table 1 shows the quantitative values of thermal lenses and their respective absorbed pump powers.

Table 1: Focal length results

P_{ABS}	15 mW	266 mW	424 mW	601 mW
$R' = -1/2A$	170,65 mm	138,12 mm	88,96 mm	64,60 mm
Focal length f_{TL}	131,39 mm	101,27 mm	60,85 mm	42,76 mm

6. CONCLUSIONS

This work presented a novel method for thermal lens characterization based on a two-wavelength speckle pattern interferometer. We have measured the thermal lens in 4% calcium aluminate glass retrieving the results from the detected wavefronts. The calculated results were obtained considering paraxial approximation.

This technique has demonstrated to be an useful and flexible method for induced lensing detection since the precision and the sensitivity of the measurement can be selected by properly tuning the lasers. The overall performance and results attest that two-wavelength DSPI is a promising method for wavefront sensing.

REFERENCES

[1] Koechner, W.,[Solid-State Laser Engineering], New York, Springer,423-486, 2006.
[2] Wetter, N. U., Maldonado, E. P. Vieira Jr, N. D., "Enhanced efficiency of a continous-wave mode-locked Nd:YAG laser by compensation of the thermally induced, polarization-dependent bifocal lens", Appl. Opt., 32:5280, 1993.
[3] Roth, M. S., Romano, V., Feurer, T., Graf, T., "Self-compensating amplifier design for cw and Q-switched high-power Nd:YAG lasers", Opt. Express, 14:2191-2196, 2006.
[4] Jiang, W.,Rao, X. Yang, Z., Ling, N., "Applications of Hartmann-Shack wavefront sensors", Proc. SPIE 6018, 6018N (2005)
[5] Barbosa, E. A., Lino, A. C. L., "Multiwavelength electronic speckle pattern interferometry for surface shape measurement", Appl. Opt. 46, 2624-2631 (2007).
[6] Pomarico, J. A., Torroba, R. D., "Focal lengths measurements using digital speckle interferometry", Opt. Comm. 141, 1-4 (1997).
[7] E. A. Barbosa, S. C. dos Santos "Refractive and geometric lens characterization through multi-wavelength digital speckle pattern interferometry" Opt. Comm. 281, 1022–1029 (2008).
[8] E. A. Barbosa, "Holographic imaging with multimode, large free spectral range lasers in photorefractive sillenite crystals", Appl. Phys. B 80, 345-350 (2005).
[9] B. Gutmann, H. Weber, "Phase unwrapping with the Branch-Cut Method: clustering of discontinuity sources and reverse simulated annealing", Appl. Opt. 38, 26:5577-5593 (1999).
[10] Verdeyen, J. T.,[Laser Electronics], Prentice Hall,Englewood Cliffs, 2008.
[11] Wang, Z., Du, C., Ruan, S.,"Thermal lens measurements in a Nd:$GdVO_4$ self-Raman laser", Opt. Laser Technol. 42, 872-877 (2010).